

SUPPLEMENTAL MATERIAL

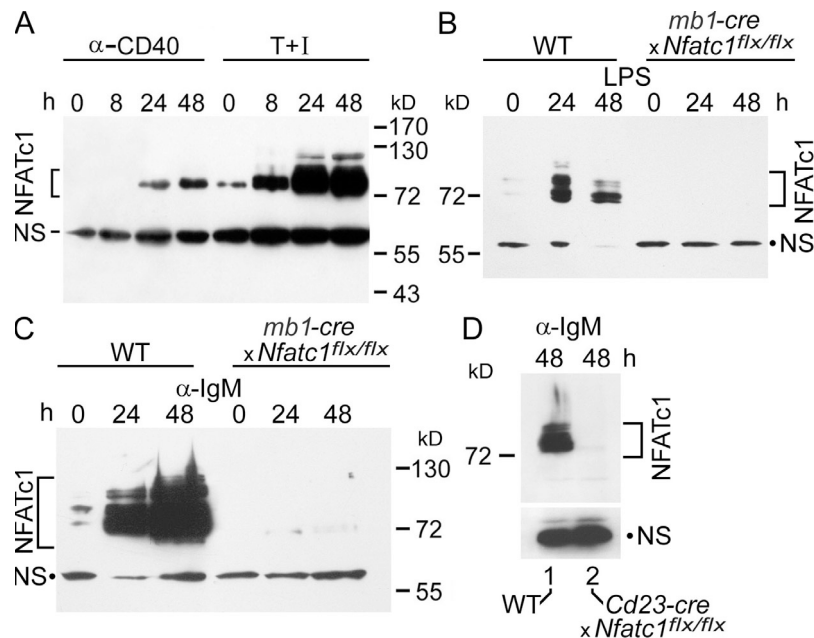
Bhattacharya et al., <http://www.jem.org/cgi/content/full/jem.20100945/DC1>

Figure S1. Detection of NFATc1 induction and its inactivation in B cells. (A) Immunoblot showing the induction of NFATc1 in splenic B cells upon induction for 0–48 h with α -CD40 (2 μ g/ml) or T+I (10 ng/ml and 0.5 μ M). (B–D) Immunoblots showing the loss of NFATc1 expression in splenic B cells from $mb1\text{-cre} \times Nfatc1^{flx/flx}$ mice and $Cd23\text{-cre} \times Nfatc1^{flx/flx}$ mice. NS, nonspecific bands. Routinely, equal loading of lanes was verified by Ponceau red staining of membranes. For each assay, three or more experiments were performed.

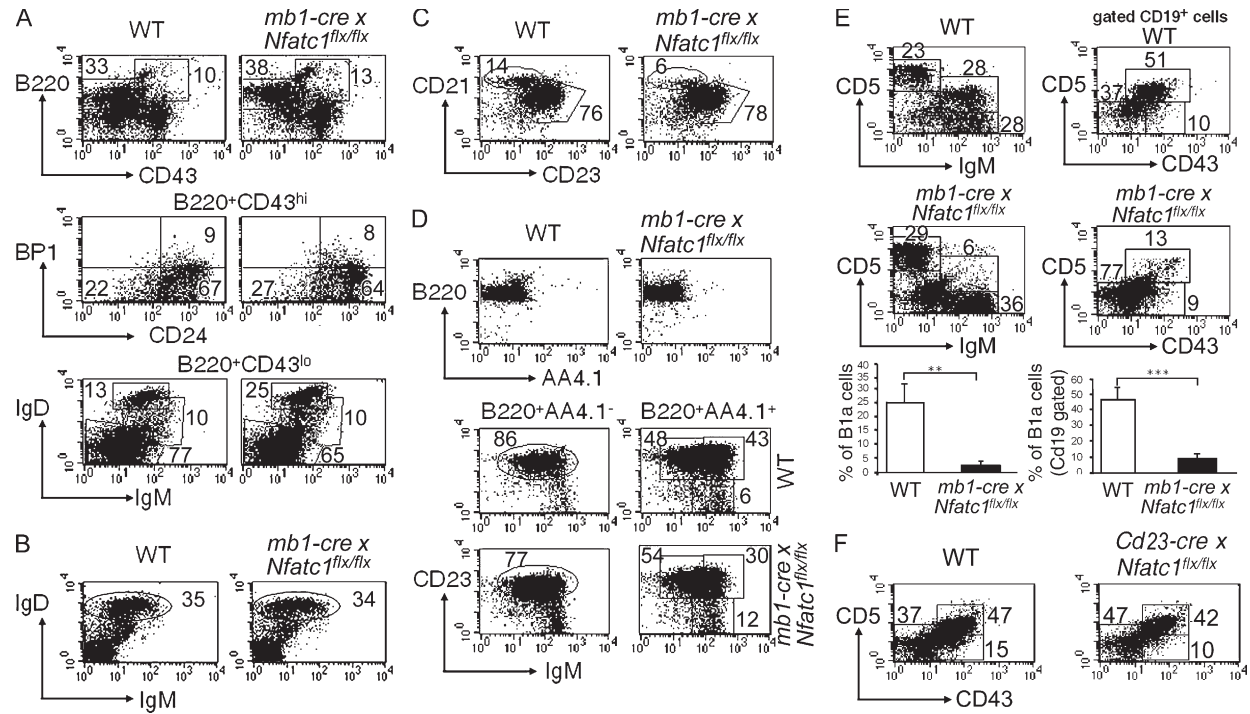


Figure S2. Development of NFATc1^{-/-} B cells in *mb1-cre* and *Cd23-cre x Nfatc1^{flx/flx}* mice. Flow cytometry of BM (A), inguinal LN (B), splenic (C and D), and peritoneal B cells (E and F). In D, splenic B cells were stained with α -B220 and α -AA4.1 to distinguish between immature (B220⁺AA4.1⁺) and mature B cells (B220⁺AA4.1⁻), followed by further stains with α -IgM and α -CD23. (E and F) Flow cytometry of peritoneal washout cells from WT and *mb1-cre* or *Cd23-cre x Nfatc1^{flx/flx}* mice, respectively. For statistical analysis, data from five (total B1a cells, above) and three (B1a cells in CD19⁺ gated cells, below) independent experiments were calculated. For all other assays, at least 3 experiments were performed.

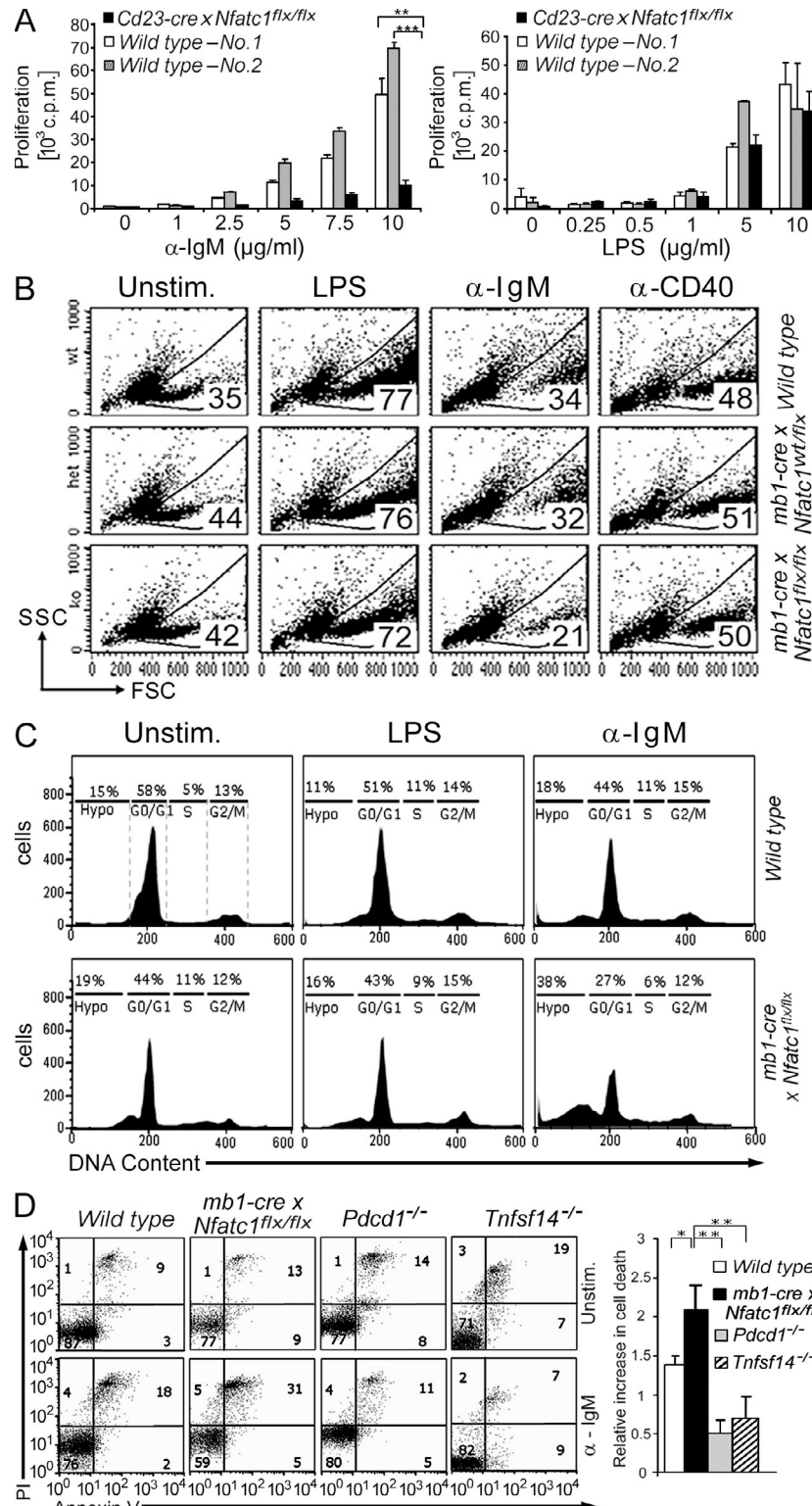


Figure S3. Impaired proliferation and survival of NFATc1^{-/-} splenic B cells. (A) [³H]thymidine incorporation assay. Naive splenic B cells from two WT mice and one *Cd23-cre x Nfatc1^{flx/flx}* mouse were stimulated with increasing concentrations of α -IgM or LPS for 72 h and incubated with [³H]thymidine for the last 16 h. (B) Forward/side scatter assay. Unstimulated splenic B cells from a WT, heterozygous *mb1-cre x Nfatc1^{wt/wt}* and homozygous *mb1-cre x Nfatc1^{flx/flx}* mouse, and B cells from the same mice stimulated with LPS, α -IgM, or α -CD40 for 40 h were measured by forward scatter (FCS) and side scatter (SSC). (C) PI stainings of WT and NFATc1^{-/-} splenic B cells incubated for 48 h in vitro for the determination of apoptotic cells and cell cycle state. (D) PD-1 and LIGHT support α -IgM-mediated AICD of splenic B cells. Flow cytometric data from one typical experiment using splenic B cells from *Pdcd1/PD-1* or *Tnfsf14/LIGHT* deficient mice (Nishimura et al., 1998; Scheu et al., 2002) are shown, and in the graph data from four (*Pdcd1^{-/-}*) or three experiments (*Tnfsf14^{-/-}*) are compiled.

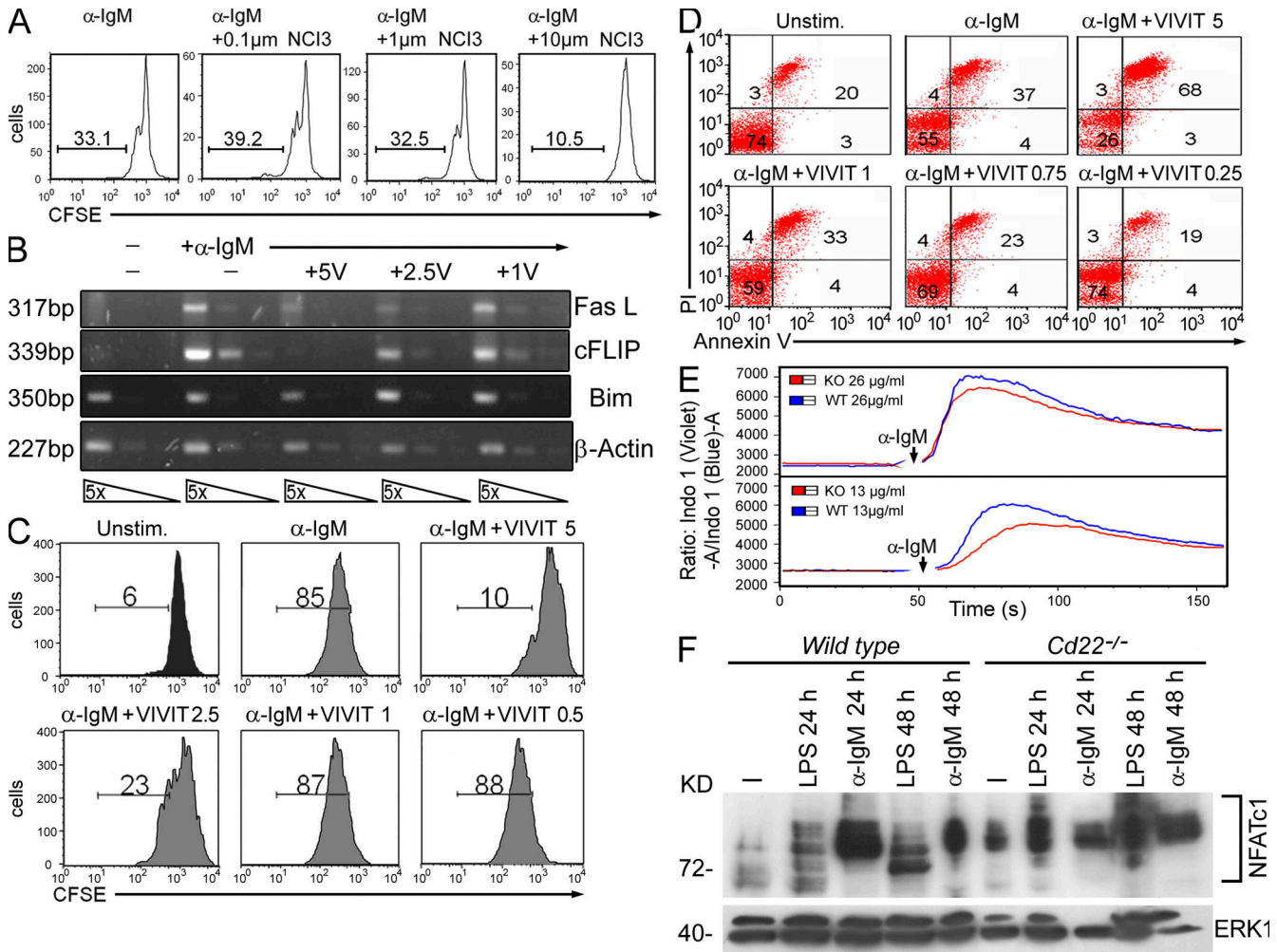


Figure S4. Effect of the Cn inhibitor NCI3 on B cell proliferation, of the NFAT inhibitor Vivit-11R on proliferation and AICD of splenic B cells, of NFATc1 ablation on Ca²⁺ flux, and of CD22 ablation on NFATc1 expression. (A) NCI3, a novel Cn inhibitor (Sieber et al., 2007), suppresses α-IgM-mediated proliferation of splenic B cells. One typical set of CFSE assays out of three is shown. (B) Semiquantitative RT-PCR assays showing the effect of 1, 2.5, and 5 μM Vivit-11R on the expression of NFAT-dependent *Fasl* and *Cflar/c-FLIP* and NFAT-independent *Actβ/β-Actin* of *Bcl2l11/Bim1* genes in splenic B cells treated with 10 μg/ml α-IgM for 24 h. (C) Impaired proliferation of splenic B cells that were left unstimulated or stimulated by α-IgM in the presence of 0.5–5 μM Vivit-11R for 3 d. Shown is one CFSE dilution assay out of 3 assays. (D) Splenic B cells were incubated with 10 μg/ml α-IgM in the absence or presence of Vivit-11R as indicated for 2 d. AICD was determined by Annexin V staining. (E) Ca²⁺ flux in B cells from *mb1-cre x Nfatc1^{fl/fl}* (KO) mice. Results of one typical experiment from more than three assays are shown. (F) Immunoblots showing the strong increase in expression of NFATc1/αA in unstimulated and LPS-treated splenic B cells from CD22^{-/-} mice.

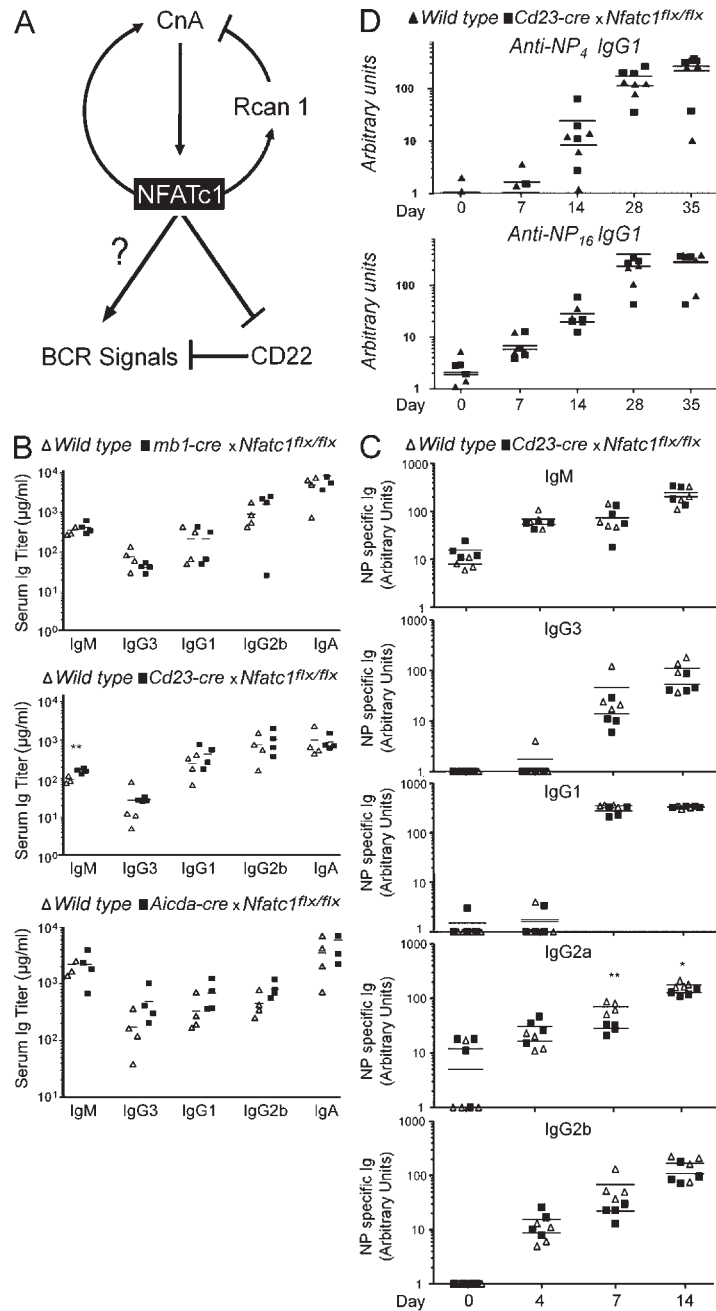


Figure S5. Model of Cn-NFATc1 network and normal Ig serum concentrations and Ig class switch in NFATc1^{-/-} B cells upon immunization with the TD antigen NP-KLH. (A) Model of a regulatory network in which NFATc1 controls its own expression through Rcan1 and Cn, and BCR-mediated signaling through CD22. It remains to be shown whether NFATc1 affects directly BCR signaling. (B) ELISA. Similar serum Ig levels in WT and in mice bearing NFATc1^{-/-} B cells. Each symbol represents a single mouse. (C) Almost normal Ig levels in sera of *Cd23-cre x Nfatc1^{flx/flx}* mice after immunization with the TD antigen NP-KLH. (D) Similar affinities of IgG1 antibodies generated in WT and *Cd23-cre x Nfatc1^{flx/flx}* mice upon NP-KLH immunization. NP₁₆-BSA-coated plates were used to measure total anti-NP-IgG1, and binding to NP₄-BSA-coated plates was used to enrich for high affinity IgG1.

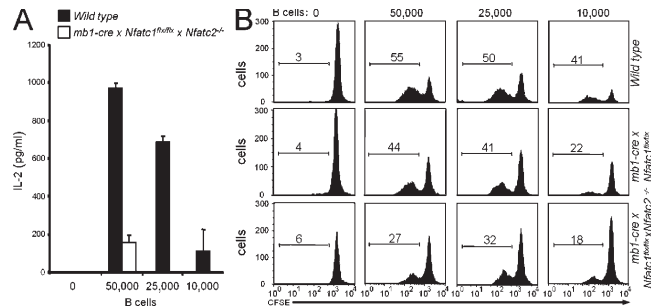


Figure S6. Poor stimulatory capacity of splenic B cells double-deficient (DKO) for NFATc1 and c2. B cells from WT, *mb1-cre x Nfatc1^{flx/flx}*, or *mb1-cre x Nfatc1^{flx/flx} x Nfatc2^{-/-}* DKO mice were treated overnight with 10 µg/ml α-IgM and 10 µM OVA₃₂₃₋₃₃₉ peptide, followed by incubation with 50,000 CFSE-stained T cells from an OTII (Barnden et al., 1998) tg mouse. Upon incubation for 3 d, the IL-2 secretion (A) and proliferation of T cells (B) was measured. Mean values (A) or one typical assay (B) from three are shown.